Search for low-Z nuclei containing massive stable particles

T. K. Hemmick,* D. Elmore,† T. Gentile,‡ P. W. Kubik, and S. L. Olsen
Department of Physics and Astronomy, The University of Rochester, Rochester, New York 14627

D. Ciampa and D. Nitz
Department of Physics, The University of Michigan–Ann Arbor, Ann Arbor, Michigan 48109

H. Kagan and P. Haas
Department of Physics, Ohio State University, Columbus, Ohio 43210

P. F. Smith
Rutherford-Appleton Laboratory, Chilton Oxon, England

B. B. McInteer
Los Alamos National Laboratory, Los Alamos, New Mexico 87545

J. Bigeleisen
Department of Chemistry, SUNY at Stony Brook, Stony Brook, New York 11794-3400
(Received 16 October 1989)

Several recent theories suggest the existence of massive stable particles that might exist in nature as remnants of the big bang. Such particles could be hidden in ordinary terrestrial matter as anomalous-mass isotopes of ordinary nuclei. A search for massive isotopes of hydrogen, lithium, beryllium, boron, carbon, oxygen, and fluorine was performed using an electrostatic charged-particle spectrometer in conjunction with a tandem accelerator. A variety of materials was sampled, including some that had heavy-particle concentrations enriched by various means. No evidence for stable isotopes with masses between 100 and 10 000 amu was found. The sensitivity of the search was greater by several orders of magnitude than the expected concentration levels, limiting the types of stable particles that could exist in this mass range.

I. INTRODUCTION

A number of recent theories suggest the existence of massive stable particles. For example, the technicolor theory for elementary particles[1] proposes the existence of a higher-order family of quarks that carry a technicolor charge, techniquarks, which are expected to have a mass in the neighborhood of 1000 amu. In this theory, technicolor singlets of three techniquarks would form technibaryons, the lightest of which would be long-lived. In the SU(4) version of the theory lifetimes of $\sim 10^{16}$ yr are expected; for the SU(5) version they are even longer, $\sim 10^{75}$ years;[2] in both cases longer than the age of the Universe. Another example is supersymmetry,[3] where every known particle has a supersymmetric partner that differs only in spin. In this model, the lightest supersymmetric-partner particle (LSP) is stable. The theory does not specify which supersymmetric particle would be the LSP and allows the possibility that it might be charged. Other candidates for stable heavy particles include strange matter,[4] integrally charged quarks,[5] and "shiny" quarks.[6]

If massive stable or long-lived particles do exist, one might expect them to be found as a low-concentration component of ordinary matter. A positively charged stable particle (hereafter referred to as X^+) would capture an electron, creating an atom with the same chemistry as hydrogen; a negatively charged particle (X^-) would bind electromagnetically to a positive nucleus with a Bohr orbit that is typically inside the nucleus. Thus, if an X^- was bound to a nucleus of atomic number Z, it would result in an atom with the same chemistry as the element with atomic number $Z-1$.

Various calculations[7,8,9] indicate that heavy particles would have been copiously produced in the big bang and remnant particles would exist in nature today at concentration levels of 10^{-10}–10^{-12} per nucleon. Bigeleisen[10] has examined the effects of an isotope's mass on its fractionation properties and the relative concentrations of isotopes in nature. He estimates that, except for hydrogen, geological concentration processes for supermassive isotopes would be similar to those for the corresponding normal mass atoms. In the case of hydrogen, relative concentrations of isotopes in the 100–10 000-amu mass range would be reduced, but by a factor of only about 100. Thus, a sensitive search for superheavy isotopes of ordinary matter would be a sensitive test of the existence of such particles.

A number of searches for anomalous-mass isotopes have been reported,[11–19] the most sensitive being the search for heavy hydrogen by Smith *et al.*[14] This experiment used electrolysis on commercial heavy water, enriching its heavy particle content relative to ordinary wa-

 ©1990 The American Physical Society

ter by a factor of approximately 10^{11}. The enriched sample was analyzed in a novel spectrometer where limits on X^+ (or $^4HeX^-$) concentrations of order 10^{-28} per nucleon were achieved for masses up to 1200 amu. Using accelerator mass spectrometry, Middleton *et al.*[15,16] have ruled out isotopes of beryllium with masses up to 93 amu at concentrations above 10^{-12} per nucleon and isotopes of oxygen up to masses of 53 amu at the 10^{-18} level. In radiochemical searches, Turkevich, Wielgoz, and Economou[17] have placed limits on carbon isotopes in the mass range from 100 to 100 000 amu of 2×10^{-15} per nucleon and Norman, Gazes, and Bennett[18] set limits on iron at the 10^{-12} level. Dick, Greenlees, and Kaufman[19] reached a similar sensitivity for sodium using atomic spectrometry techniques.

We report here the results of a search for heavy isotopes of hydrogen, lithium, beryllium, boron, carbon, oxygen, and fluorine, using a charged-particle spectrometer constructed of only electrostatic devices at the University of Rochester's Nuclear Structure Research Laboratory (NSRL). An all-electrostatic system transmits particles independently of their masses, an ideal condition for searching for exotic particles of unknown mass. This work is the subject of a Ph.D. thesis[20] and preliminary results were reported in Ref. 21.

II. EXPERIMENTAL CONFIGURATION

An overall view of the spectrometer, which is described in Ref. 22, is shown in Fig. 1. A cesium sputter source produced negative ions that were accelerated through 150 kV and sent directly into a tandem electrostatic accelerator. At the terminal of the accelerator, which was biased at +5 MV, the beam passed through a 5-μg/cm^2 carbon foil stripper. Positive ions emerging from the foil were further accelerated to the high-energy end of the accelerator where they were focused by an electrostatic quadrupole doublet located between the last acceleration tube and the exit of the accelerator's pressure vessel. At the exit point, the selected beam component was deflected through an angle of 1.3° by a pair of electrostatic plates onto a set of tantalum slits, with a second stripping foil between them. Ions emerging from the foil were bent through 20° by an electrostatic analyzer and focused onto the entrance window of the detector by a second electrostatic quadrupole doublet.

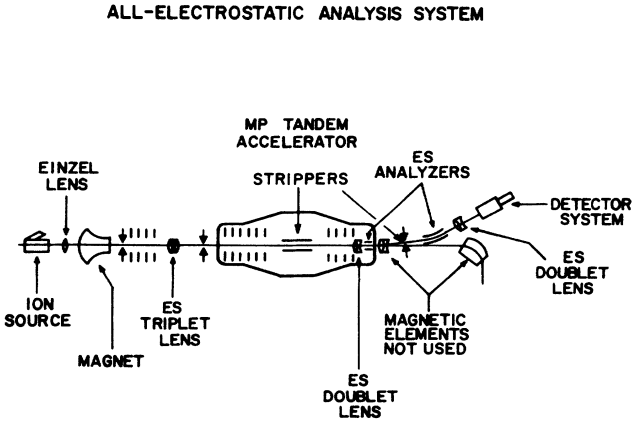

FIG. 1. A schematic diagram of the Rochester all-electrostatic mass-independent accelerator mass-spectrometry system.

Low-mass ions were rejected by the beam transport system by (i) selecting $q=1^+$ charge states from each stripping foil, (ii) weak sweeping magnets placed at the entrance and exit of the beam line, and (iii) absorbers placed at the entrance of the detector. We discuss each item separately.

(i) Stripping yields. When an ion emerges from a stripping foil, its most probable charge state is a function of the ion's velocity. Since heavier isotopes have lower velocities than lighter ones of the same energy, they tend to strip to lower-charge states. The spectrometer was tuned to accept $E/q=10$ MV ions ($q=1^+$) from both stripping foils thus rejecting ordinary ions, which mostly strip to higher-charge states. Calculations and measurements indicated that, for the X^- searches the rejection of low-mass ions provided by the strippers was about 10^{-7}, while the heavy-ion transmission remained at about 10%. In the case of the heavy hydrogen (X^+) search the strippers provided no significant rejection.

(ii) Sweeping magnets. Sweeping magnets, placed between the injector and the entrance to the accelerator and between the last set of steerers and the detector, were used to provide additional low-mass rejection. In the X^+ search, the injection magnet was set to 26 G and the detector magnet at 200 G. This deflected ordinary hydrogen isotopes from the system but had no effect for ions with masses above 100 amu. In the case of the X^- searches, only the 200-G detector sweeping magnet was used.

(iii) Absorbers. High-Z elements have a considerably higher dE/dx and shorter range in matter than the ions for which we are searching. Backgrounds from high-Z ions that were not rejected by the strippers or magnets were eliminated by absorbers placed before the entrance to the detector. For the X^- search this absorber was a gas cell; for the X^+ search it was a 250-μm Zr foil. In all cases, the absorber material was such that it ranged out background ions while allowing supermassive isotopes to pass through.

Ions were detected and their masses determined by a multiplate gas ionization detector that measured differential energy loss, range, and total energy. In the detector, which is shown in Fig. 2, electrons drift through a Frisch grid to split-anode collection plates. The charge collected on each plate is a measure of the energy loss in a fixed region of the gas. The total energy was determined from the induced pulse on the cathode. The device has an energy resolution that is typically 1%. The total information from the counter provides resolution sufficient to separate neighboring isobars. There was a time-of-flight (TOF) counter system placed upstream of the gas counter that was primarily used for calibration and diagnostic purposes.

The energy loss for heavy particles was estimated using the formalism of Ziegler.[23] For the nuclear stopping power, the formula derived by Wilson[24] was used. For

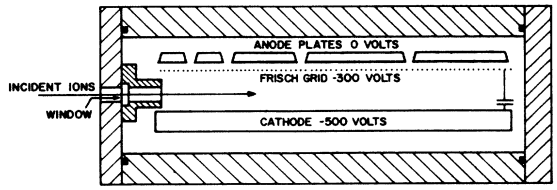

FIG. 2. The split-anode gas ionization detector. Ions enter the gas-filled region though a thin window from the left. Ionization electrons drift upward through the Frisch grid and are collected on the anode plates. The total energy is determined from the induced pulse on the chamber bounded by the cathode and grid.

the electronic stopping power, the Lindhardt-Scharff[25] results for low velocities, solved in closed form using a Thomas-Fermi calculation for the electron charge density, were interpolated to the standard Bethe-Bloch formula[26] for higher velocities with a quadratic interpolation function; the end points of the interpolation were found by fitting to published data.

To verify the mass independence of the beam-transport system, an alloy sample of Be, Cu, and Au was prepared. The source and stripper yields and the accelerator's transmission of each element were initially determined for each element separately with the injection system operating in a conventional mass-spectrometry mode. These measurements were used to predict the relative simultaneous yields of the three elements when they were injected into the system using the mass independent mode. The TOF system was used to identify the three elements. The measured relative yields, summarized in Table I, were close to the expected values. Small variations in the optimum beam tunes for these three elements were identified as being due to small differences in the energy losses in the two stripper foils and to small residual magnetic fields at the low-energy end of the accelerator. These effects, which are just measurable for normal mass ions, have little effect on the high-mass, low-Z ions that are the subject of the search reported here. During normal operation the acceptance was made to be much broader than these small differences in tune. Transmission measurements of the three elements from the Be-Cu-Au alloy were repeated periodically during the course of the experiment to verify the mass independence of the beam transport system.

We measured the stripping-foil charge-state yields for various ion beams for 5 and 10 MeV, with the injection system operated in the conventional mass spectrometer mode. The measurements, shown in Figs. 3(a) and 3(b), agree well with the empirical formulas of Ref. 27 and indicate that the light-ion rejection obtained by selecting 1^+ charge states from both stripping foils is a factor of about 10^7.

During the data collection for the X^- searches, a routine was established for checking that the beam line elements were properly tuned by turning off the sweeping magnet and measuring the counting rate for normal mass isotopes. In addition, we checked that the yield of 1^- ions from the source was stable. This procedure was repeated every 40 min. In the case of the X^+ search, residual magnetic fields in the low-energy end of the accelerator required us to reset the injection steerers in order to establish a D^+ beam, which was used to check the tune of the high-energy beam elements. As a part of this procedure, we established the source yield by measuring the pressure in the ion source; the D^- ion current was found to be proportional to this pressure to good accuracy. Because this procedure required the injection steerers to be reset, it was a more time-consuming process than that used for the X^- searches and was therefore done only every four hours.

Occasionally during the X^- searches, a small pinhole developed in the terminal stripping foil, resulting in an anomalously large yield of $q=1^+$ normal ions. During

TABLE I. Results of tests of the mass independence of the beam transport using the Be-Cu-Au alloy sample.

	Beryllium	Copper	Gold
Source current (nA)	11	1200	625
Transmission efficiency	19.5%	3.8%	1%
1^+ stripper yield	1.5×10^{-3}	1.0×10^{-5}	1.0×10^{-5}
Relative count rates			
Predicted:	1000	199	20
Observed:	1000	146	16

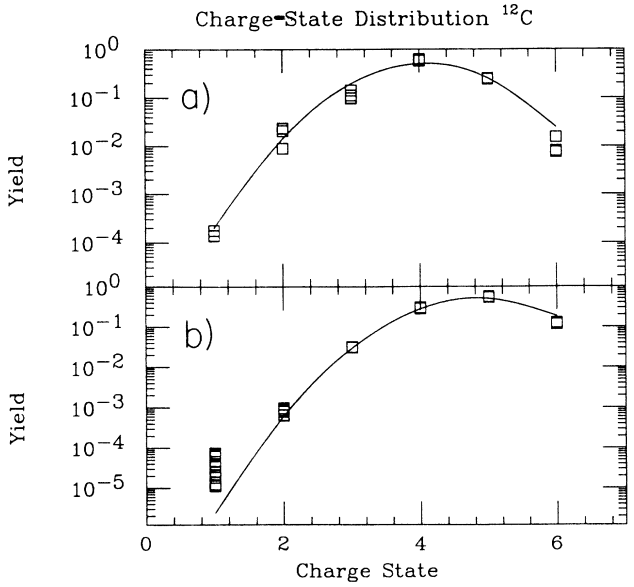

FIG. 3. The distribution of charge states of carbon ions passing through a thin (5 $\mu g/cm^2$) carbon foil stripper at (a) 5 MeV and (b) 10 MeV. The solid curve is a prediction based on semi-empirical formulas. The high yield for the 1^+ charge state at 10 MeV results from incident 1^+ ions passing through a small hole in the foil.

the experiment, the TOF system was used as a continuous monitor of the background $q=1^+$ yields. The abrupt increase in the TOF rate made the occurrence of a defect in the foil easy to detect and correct. The data collected around the times that damaged foils were detected were rejected.

III. SAMPLE PREPARATION

In the searches for heavy isotopes of hydrogen, carbon, and oxygen, we increased the sensitivity level by doing a bulk reduction on the samples before subjecting them to analysis. In the case of hydrogen, we used commercial deuterium gas with a heavy isotope enrichment factor of 2×10^4, heavy-water (D_2O) samples remaining from the search reported in Ref. 14, prepared from lake water, with enrichment factors of 10^6, 10^8, and 10^9, and an unenhanced sample of seawater taken from a depth of 3 km. An enriched carbon sample was prepared at the ^{13}C enrichment plant at Los Alamos. Carbon monoxide was fractionated via a low-temperature distillation procedure. Approximately one ton of carbon of petrochemical origin was processed to produce a final sample that had an enrichment of high-mass carbon isotopes of a factor of 10^5. For the oxygen search we used a commercial ^{18}O sample, obtained in the form of $H_2{}^{18}O$, that had a heavy isotope enrichment factor of 416. Chemical reagent samples of Li, Be, B, and F were used in the heavy isotope searches for these elements.

The enriched samples required further processing to produce forms suitable for use in the ion source. The enriched ^{13}CO sample was chemically processed to trap the carbon isotopes in iron balls that were used in the ion source. Since the oxygen component of the enriched D_2O samples would produce too much beam current for the accelerator, it was removed by the chemical processes $D_2O+Mg\rightarrow MgO+D_2$. The D_2 was bled into the ion source through a needle valve. The $H_2{}^{18}O$ sample was converted to solid $Ca^{18}O$ by the reaction $H_2{}^{18}O+Ca\rightarrow Ca^{18}O+H_2$.

IV. DATA ANALYSIS

Candidates for heavy isotopes were selected according to the dE/dx signals that were measured by the split anode gas ionization detector. In the case of the X^+ search, this was simplified by the fact that heavy-hydrogen isotopes would have a shorter range in the gas counter than the ordinary isotopes ^1H and ^2H and, thus, would have larger signals on the first few plates of the counter. The expected range in the counter increases with mass such that an $M=100$ amu isotope would stop under the second plate and an $M=10\,000$ amu isotope would stop under the third plate. We selected events in which there were no signals recorded beyond the fourth plate of the counter. In Figs. 4(a) and 4(b) we show a scatter plot for δE_1 vs δE_2 (δE_2 vs δE_3) for the detected ions that did not penetrate beyond the fourth plate for the most highly concentrated heavy-hydrogen sample. The expected location of signals from heavy isotopes is shown as a function of mass by the line in each scatter plot. There are no events consistent with being X^+ candidates for masses between 100 and 10 000 amu.

The selection for X^- candidates was more complicated since, in this case, high-mass isotopes would have longer ranges and smaller pulse heights than their low-mass counterparts. In Figs. 5(a) and 5(b) we show a scatter plot of E_{tot} vs δE_1 (δE_2 vs δE_1) for the enriched ^{13}C sample. Here there is clearly more background than in the X^+ search. For each event, we used six measured quantities (E_{tot} and δE_i, $i=1$ to 5) and computed the closest distance in the six-dimensional E_{tot}, δE_i hyperspace between each measured point and the curve corresponding to the expected position for isotopes of mass ranging from 100 to 10 000 amu. We selected events that were within 2 MeV of this curve. (Our resolution in this quantity, determined from applying the same technique to known isotopes, was typically less than 0.8 MeV.) Some events passed these criteria. Their origin was traced to α-particle radiation from a low-level ^{241}Am con-

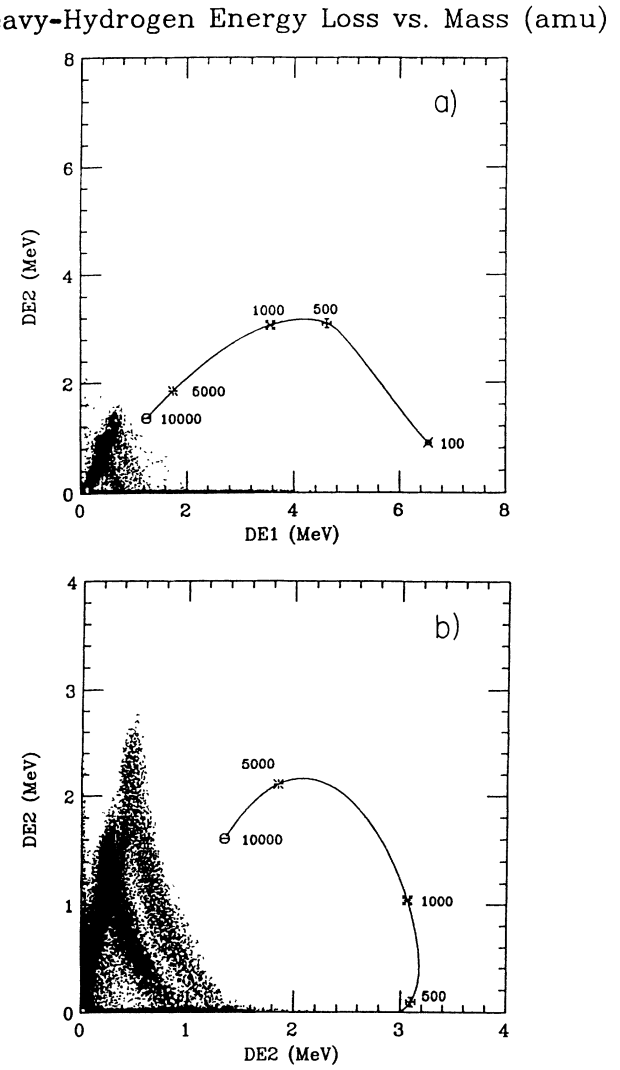

FIG. 4. Scatter plots of (a) δE_1 vs δE_2 and (b) δE_2 vs δE_3 for the hydrogen sample that was enriched by a factor of 10^9. The predicted locations for heavy particles are shown as a function of mass (in amu).

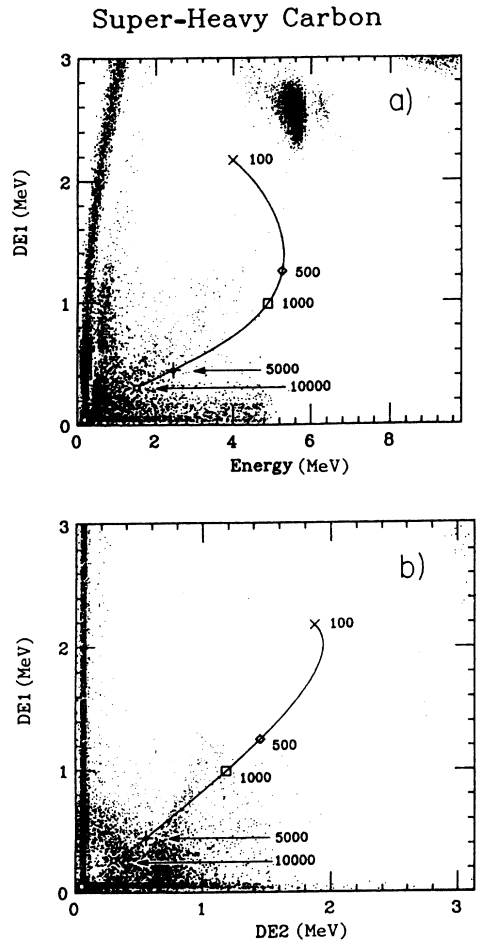

FIG. 5. Scatter plots of (a) $E_{\rm tot}$ vs δE_1 and (b) δE_1 vs δE_2 for the enriched carbon sample. The predicted locations for heavy particles are shown as a function of mass (in amu).

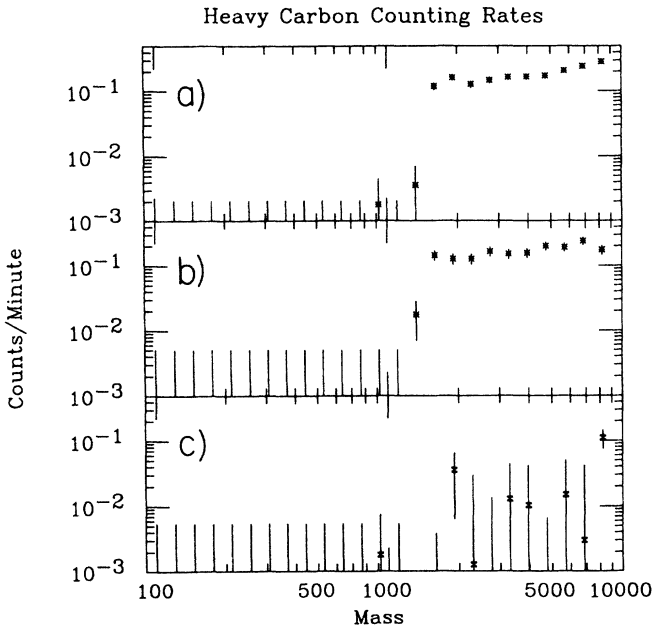

FIG. 6. The counting rate as a function of inferred mass for (a) the enriched carbon sample and (b) no sample (valve closed). The background is attributed to a ^{241}Am contamination in the detector and accounts for all of the observed events as can be seen from (c) the background subtracted distribution.

tamination of the detector container that survived the cleaning procedures that preceded the experiment. Figure 6(a) shows the rate of events as a function of inferred mass for the ^{13}C search; Fig. 6(b) shows the same analysis for data taken with the detector completely shielded from the beam. The two spectra are similar; the shielded spectrum is used to perform a background subtraction, with the residual spectrum shown in Fig. 6(c). In no case did the subtracted spectra show a count rate that was more than two standard deviations above zero. These subtracted count rate spectra were used to establish concentration limits for X^- particles.

Concentration limits were determined from the relation

$$C(m)=\frac{n_{2\sigma}}{\epsilon(m)\gamma_s}\int\frac{I(t)}{e}dt\ ,$$

where

$$\epsilon(m)=\tau Y(m_h)\left[\frac{N^-(m_h)}{N^-(m_l)}\right]\ .$$

Here, $\epsilon(m)$ is the product of all of the mass-dependent efficiencies, γ_s is the enrichment of the sample, $\int I(t)$ is the integrated source current over the data sampling live time and $n_{2\sigma}$ is the two-standard-deviation (90%-C.L.) upper limit on the number of candidate events. The efficiency has three components: τ is the transmission efficiency; $Y(m_h)$ is the product of the relative stripping efficiency for the two stripping foils for heavy and low-mass ions; and $N^-(m_h)/N^-(m_l)$ is the ratio of negative-ion formation rates for heavy and low-mass ions.

Transmission losses were dominated by electron stripping from negative ions in the residual gas near the entrance of the accelerator. These losses have been measured for normal ions by Lund[28] and are found to range from 10% for $^{16}O^-$ to 75% for $^{197}Au^-$. Charge changing cross sections are expected to factorize as $\sigma=f(Z)g(v/v')$, where $v'=e^2/h=0.007c$ is a velocity that is typical of the outermost electron in an atom. Measurements of $g(v/v')$ (Ref. 29) indicate that it has a broad maximum at $v/v'\sim 1$ and drops by an order of magnitude for $v/v'\sim 10$. For lower values of v/v', this quantity is down by a factor of about 3 at $v/v'\sim 0.1$. In the entrance region of the accelerator, ordinary ions have values of v/v' that range from about 2 to 10, while the heavy-mass isotopes that we are searching for have v/v' values ranging from 0.024 to 1.0. Thus, we expect relative transmission efficiencies to be the same to within one order of magnitude. To be conservative, we assign the heavy isotopes a 10% transmission efficiency relative to that for the ordinary ions.

For stripping efficiencies, we use the empirical formulas of Ref. 27 to extrapolate to velocities corresponding to

high-mass isotopes. These formulas reproduced our measured stripping yields reasonably well.

The rate for negative ion production can be written as $N^-(m)=Y(m)S^-(m)$, where $Y(m)$ is the sputtering yield and $S^-(m)$ is the negative-ion formation probability. For the sputtering yield, we use the empirical formula of Matsunami *et al.*,[30] which indicates a relative loss of about an order of magnitude at mass 10 000. For $S^-(m)$, we use the theory of Norskov and Lundquist,[31] which agrees well with experimental observations of Yu[32] and Vasile.[33] In this model, $S^-(m) \propto \exp(-\beta\sqrt{m})$; for β, we use the value that was determined for $^{16}O^-$ in Ref. 31.

V. RESULTS

We find no evidence for anomalous isotopes of terrestrial H, Li, Be, B, C, O, and F in the mass range from 100 to 10 000 amu. We establish concentration limits as listed in Table II, and shown in Fig. 7. For the case of heavy hydrogen, we only show the results for the seawater sample and the heavy-water sample that was enriched by a factor of 10^9. No candidates were found in any of the other water samples; the concentration limits derived from them are similar to those presented degraded by the relative enhancement factors. Except for the lower mass range of hydrogen, these limits are the most sensitive reported to date. In the case of hydrogen, our results set the most stringent concentration limits for masses in the range 1200 to 10 000 amu.

The concentration limits are well below the theoretically expected level of 10^{-10} to 10^{-12} heavy particles per nucleon. Geochemical processes are not expected to dramatically change the concentration of heavy isotopes in matter. For example, in Bigeleisen's model,[10] the ratio of maximum fractionation effects for different mass isotopes, α, has a mass dependence given by

$$\ln(\alpha) \propto \left[\frac{1}{m_l} - \frac{1}{m_h}\right],$$

where m_l and m_h are the light and heavy masses.[10] This relation was used to estimate the maximum chemical fractionation of anomalous-mass isotopes in nature by fixing the proportionality constant to match the measured values for known isotopes. Estimates of these effects for heavy isotopes for several elements are given in Table III. Fractionation effects for hydrogen are the most severe, the concentration of heavy-mass isotopes being suppressed by about a factor of 100; for carbon, it is less than 10. Smith and Bennett[34] have considered the effects of oceanic settling of heavy-mass isotopes. They find an equilibrium time constant of $>10^8$ years, much longer than the mixing rate for the oceans, which is of order 10^3 years. Thus, heavy isotopes in ocean water would remain homogenized.

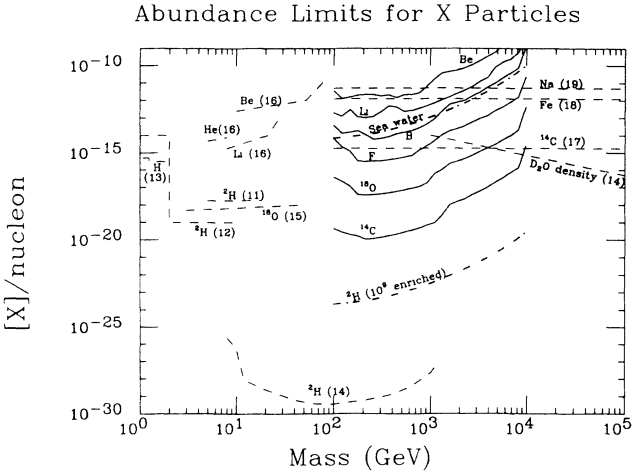

FIG. 7. Measured concentration limits for X particles in various elements. Previous results are shown with dashed lines with the corresponding reference number indicated in parentheses. The present results for X^- particles are shown with solid lines, and for X^+ particles as dotted-dashed lines. For hydrogen, only the results for the seawater sample and the sample that was enriched by a factor of 10^9 are shown.

The difference between our observed concentration limits for hydrogen and the predicted concentrations for X^+ particles are many more orders of magnitude lower than can be explained by fractionation processes. Thus we conclude that stable X^+ particles of the type discussed in Refs. 7 and 8 do not exist in the mass range from 100 to 10 000 amu. The case for a negatively charged X^- particle, which might preferentially attach to some particular nucleus, is somewhat more ambiguous. Nevertheless, our limits, covering a variety of nuclear species, are well below predicted levels (by a factor of 10^8 in the case of carbon). Thus, a stable X^- particle in the same mass range must be considered to be extremely un-

TABLE II. Abundance limits (at the 2σ level) for heavy isotopes established by this experiment. In the case of H, C, and O, sample enrichment techniques were used.

Mass (amu)	H	Li	Be	B	C	O	F
100	2×10^{-24}	2×10^{-13}	4×10^{-12}	4×10^{-14}	4×10^{-20}	4×10^{-17}	7×10^{-15}
500	9×10^{-24}	3×10^{-13}	2×10^{-12}	1×10^{-14}	2×10^{-20}	6×10^{-17}	5×10^{-16}
1000	3×10^{-23}	6×10^{-13}	1×10^{-11}	6×10^{-14}	8×10^{-20}	4×10^{-17}	4×10^{-15}
5000	2×10^{-21}	9×10^{-11}	1×10^{-9}	1×10^{-11}	3×10^{-17}	4×10^{-15}	3×10^{-13}
10 000	3×10^{-20}	7×10^{-10}	7×10^{-9}	8×10^{-11}	2×10^{-16}	3×10^{-14}	2×10^{-12}

TABLE III. Estimates of $\alpha^{-1}(M_X)$, the maximum change in concentration of a mass M_X isotope relative to that of the common isotope, due to geological fractionation. The theory (Ref. 10) uses known relative abundances of ordinary isotopes (references) to extrapolate to heavier masses. (All masses are in amu.)

Element	Reference masses	$\alpha^{-1}(M_X=10)$	$\alpha^{-1}(M_X=100)$	$\alpha^{-1}(M_X=1000)$	$\alpha^{-1}(M_X=\infty)$
Hydrogen	1,2	0.015	0.010	0.010	0.010
Carbon	12,13		0.31	0.28	0.27

likely. The situation for neutral massive stable particles is more complex. It is discussed in detail in Ref. 9.

ACKNOWLEDGMENTS

We gratefully acknowledge K. Nishiizumi for providing the deep seawater sample and J. D. Bowman for the loan of the time-of-flight detectors. We thank T. Haelen of the University of Rochester's 130-inch Cyclotron Laboratory for his help in designing and installing the all-electrostatic beam line and W. Jones of the Chemistry Department for his assistance in the chemical processing of the enriched water samples. We also wish to express our thanks to the staff of the NSRL for their aid in the operation of the experiment. N. Conrad helped in the preparation of the samples and R. Teng helped maintain the ion source and detector. This work has been supported by the United States Department of Energy and the National Science Foundation.

*Current address: A. W. Wright Nuclear Structure Laboratory, Yale University, New Haven, CT 06511.

†Current address: Physics Department, Purdue University, West Lafayette, IN 47907.

‡Current address: Lincoln Laboratories, Massachusetts Institute of Technology, Cambridge, MA 02139.

[1]E. Farhi and L. Susskind, Phys. Rep. **74C**, 277 (1981).

[2]R. S. Cahn and S. L. Glashow, Science **213**, 607 (1981).

[3]J. Wess and B. Zumino, Nucl. Phys. **B70**, 39 (1974).

[4]E. Witten, Phys. Rev. D **30**, 272 (1984); E. G. Blackman and R. L. Jaffe, Nucl. Phys. **B324**, 205 (1989).

[5]M. Y. Han and Y. Nambu, Phys. Rev. **139**, B1006 (1965).

[6]F. Wilczek and A. Zee, Phys. Rev. D **16**, 860 (1977).

[7]S. Wolfram, Phys. Lett. **82B**, 65 (1979).

[8]C. B. Dover, T. K. Gaisser, and G. Steigman, Phys. Rev. Lett. **53**, 1117 (1979).

[9]D. A. Dicus and V. L. Teplitz, Phys. Rev. Lett. **44**, 218 (1980).

[10]J. Bigeleisen, Isot. Chem. Principles **11**, 1 (1975).

[11]T. Alvager and R. A. Naumann, Phys. Lett. **24B**, 647 (1967).

[12]R. Muller, L. A. Alvarez, W. R. Holley, and E. J. Stephenson, Science **196**, 521 (1977).

[13]R. N. Boyd, D. Elmore, D. Nitz, S. Olsen, E. Sugarbaker, and G. Warren, Phys. Lett. **72B**, 484 (1978).

[14]P. F. Smith, J. R. J. Bennett, G. J. Homer, J. D. Lewin, H. E. Walford, and W. A. Smith, Nucl. Phys. **B206**, 333 (1982).

[15]R. Middleton, R. W. Zurmuhle, J. Klein, and R. V. Kollarits, Phys. Rev. Lett. **43**, 429 (1979).

[16]J. Klein, R. Middleton, and W. E. Stevens, in *Proceedings of the Symposium on Accelerator Mass Spectroscopy* (Argonne National Laboratory Report No. ANL/PHY-81-1, 1981), p. 136.

[17]A. Turkevich, K. Wielgoz, and T. E. Economou, Phys. Rev. D **30**, 1876 (1984).

[18]E. B. Norman, S. B. Gazes, and D. A. Bennett, Phys. Rev. Lett. **58**, 1403 (1987).

[19]W. J. Dick, G. W. Greenlees, and S. L. Kaufman, Phys. Rev. Lett. **53**, 431 (1984).

[20]T. K. Hemmick, Ph.D. thesis, University of Rochester, 1988.

[21]T. K. Hemmick, D. Elmore, P. W. Kubik, S. L. Olsen, T. Gentile, D. Nitz, D. Ciampa, H. Kagan, P. Haas, P. F. Smith, B. B. McInteer, and J. Bigeleisen, Nucl. Instrum. Methods **B29**, 389 (1987).

[22]D. Elmore, P. W. Kubik, T. Hemmick, R. Teng, H. Kagan, P. Haas, R. N. Boyd, R. Turner, D. Nitz, D. Ciampa, S. L. Olsen, T. Gentile, and T. Haelen, Nucl. Instrum. Methods **B10**, 738 (1985).

[23]J. F. Ziegler, *The Stopping Power and Ranges of Ions in Matter* (Pergamon, New York, 1980); J. F. Ziegler, J. P. Biersack, and U. Littmark, *The Stopping Power and Ranges of Ions in Matter* (Pergamon, New York, 1985).

[24]W. D. Wilson, L. G. Haggmark, and J. P. Biersack, Phys. Rev. B **15**, 2458 (1977).

[25]J. Lindhard and M. Scharff, Dan. Mat. Fys. Medd. **27** (No. 15), 1 (1953).

[26]H. Bichsel, in *American Institute of Physics Handbook,* 3rd ed. (McGraw-Hill, New York, 1972).

[27]I. S. Dmitriev and V. S. Nikolaev, Zh. Eksp. Teor. Fiz. **47**, 615 (1964) [Sov. Phys. JETP **20**, 409 (1965)].

[28]T. S. Lund, Rev. Phys. Appl. **12**, 1341 (1977).

[29]S. K. Allison and M. Garcia-Munoz, in *Atomic and Molecular Processes,* edited by D. R. Bates (Academic Press, New York, 1962).

[30]N. Matsunami, Y. Yamamura, Y. Itikawa, N. Itoh, Y. Kazumata, S. Miyagawa, K. Morita, R. Shimizu, and H. Tawara, At. Data Nucl. Data Tables **31**, 1 (1984).

[31]J. K. Norskov and B. I. Lundqvist, Phys. Rev. B **19**, 5661 (1979).

[32]M. L. Yu and N. D. Lang, Nucl. Instrum. Methods **B14**, 403 (1986).

[33]M. J. Vasile, Phys. Rev. B **29**, 6046 (1984).

[34]P. F. Smith and J. R. J. Bennett, Nucl. Phys. **B149**, 525 (1979).